Macromolecules
ARTICLE

Macromolecules **2009**, *42*, 6023–6030 **6023**
DOI: 10.1021/ma900898m

Polymers of Intrinsic Microporosity Derived from Novel Disulfone-Based Monomers†

Naiying Du,‡ Gilles P. Robertson,‡ Ingo Pinnau,§ and Michael D. Guiver*,‡

‡*Institute for Chemical Process and Environmental Technology, National Research Council of Canada, Ottawa, Ontario K1A 0R6, Canada, and* §*Membrane Technology and Research, Inc., 1360 Willow Road, Suite 103, Menlo Park, California 94025-1516.* † *NRCC Publication No. 51690.*

Received April 24, 2009; Revised Manuscript Received June 1, 2009

ABSTRACT: The synthesis of three novel disulfone-based monomers from readily available hexafluorobenzene and thiols for the preparation of homopolymers and copolymers of intrinsic microporosity (PIMs) is described. The disulfonyl-based PIMs derived from 5,5′,6,6′-tetrahydroxy-3,3,3′,3′-tetramethylspirobisindane (TTSBI) with tetrafluoroterephthalonitrile (TFTPN) and disulfone-based monomers were prepared at high temperature (160 °C) within 1 h. Three new copolymers (monomer molar ratio of TTSBI and disulfone-based monomers = 3:1) show a good combination of properties, such as excellent film-forming characteristics and gas transport properties. Compared with a previously reported microporous nitrile-based homopolymer, referred to as PIM-1, the present sulfone-based copolymers have higher gas selectivities for O_2/N_2 and CO_2/N_2, while showing some reduction in pure-gas permeabilities. The relationship between the structure and gas permeation behavior of the copolymers is discussed.

Introduction

In recent decades, polymeric microporous materials have had a great impact on academic research and industrial applications. To date, several types of microporous polymeric materials have been reported, for example solvent-swollen cross-linked polymers (e.g., hyper-cross-linked polystyrenes),[1,2] rigid polymer networks,[3−8] rigid non-network polymers, such as poly(1-trimethylsilyl-1-propyne),[9,10] certain polyimides,[11,12] a number of fluorinated polymers,[13] or polymers with bulky structural units,[14,15] and especially a class of polymers with high microporosity obtained via thermal rearrangement.[16] Recently, Budd and coworkers described a novel class of high free volume polymeric microporous materials termed "polymers of intrinsic microporosity" (PIM) whose rigid and randomly contorted structures decrease chain packing efficiently in the solid state. Hence, these materials have gained considerable attention for use in heterogeneous catalysis,[3,17a] membrane separations,[17b,18] and hydrogen storage[4,19−21] and as adsorbents for organic compounds.[3,22]

The most commonly reported such material having high molecular weight, termed PIM-1, is prepared from commercially available 5,5′,6,6′-tetrahydroxy-3,3,3′,3′-tetramethylspirobisindane (TTSBI) and 2,3,5,6-tetrafluoroterephthalonitrile (TFTPN) by an efficient double aromatic nucleophilic substitution (S_NAr) polycondensation. However, only a few PIM structures with high molecular weight have been reported to date[23−27] due to (1) the limited choice of available monomers and (2) sufficient reactivity of available monomers in producing sufficiently high molecular weight polymers. The latter is an important consideration in using these materials for membrane gas separation, where materials with high molecular weight are required for preparation of thin-film composite membranes and for fabricating free-standing isotropic films. Therefore, it is highly desirable to expand the spectrum of high molecular weight PIMs having new structures derived from different monomers for the purpose of determining the structure−gas permeability properties of this unique class of materials.

According to previous studies on polymer structures, the incorporation of phenylsulfonyl ($-SO_2Ar$) is commonly considered to improve gas separation properties. In general, the presence of $-SO_2-$ raises T_g through increasing the rigidity of the polymer chain. It tends to reduce fractional free volume (FFV) and permeability but increases selectivity.[28] In our recent work,[26] PIM copolymers derived from a monomer containing $-CF_3$ and $-SO_2C_6H_5$ side groups exhibited high selectivity coupled with a permeability that combines to exceed the Robeson upper bound for O_2/N_2. These results suggest that the $-CF_3$ and $-SO_2C_6H_5$ groups on the polymer main chains exert a considerable influence on the gas transport properties. The present work focuses on the synthesis of new PIMs derived from sulfone monomers and studies the effect of the side groups on microporosity for gas permeation behavior. The new PIM copolymers were prepared from three different tetrafluorodisulfone monomers (Scheme 1), such that the resulting PIM copolymers contain bulky, rigid groups. In particular, we wished to determine whether the presence of such groups increases selectivity due to a further enhancement in chain rigidity and space filling. Although the syntheses of tetrafluorodithio compounds **1a** and **1c**, which are monomer precursors, and tetrafluorodisulfonyl compound **2a** were reported many years ago,[29−31] structural characterization and proof of structure are lacking for the latter compound. Furthermore, compound **2a** has not previously been utilized as a monomer. Herein, we report the synthesis and purification of three new disulfonyl monomers (**2a**−**2c**), and the structure and characterization of 1,2,4,5-tetrafluoro-3,6-bis(methoxy-4-phenylsulfonyl)benzene (**2b**) and 1,2,4,5-tetrafluoro-3,6-bis(ethylsulfonyl)benzene (**2c**) are described for the first time. In addition, the resulting disulfone-based PIMs present a new class of microporous polymers, and we report the structures, synthesis, and physical properties, including the gas separation properties of this new class of PIMs.

*Corresponding author. E-mail: Michael.guiver@nrc-cnrc.gc.ca.

Published on Web 07/01/2009

Scheme 1. Synthetic Route for the DSPIM1−3 Series[a]

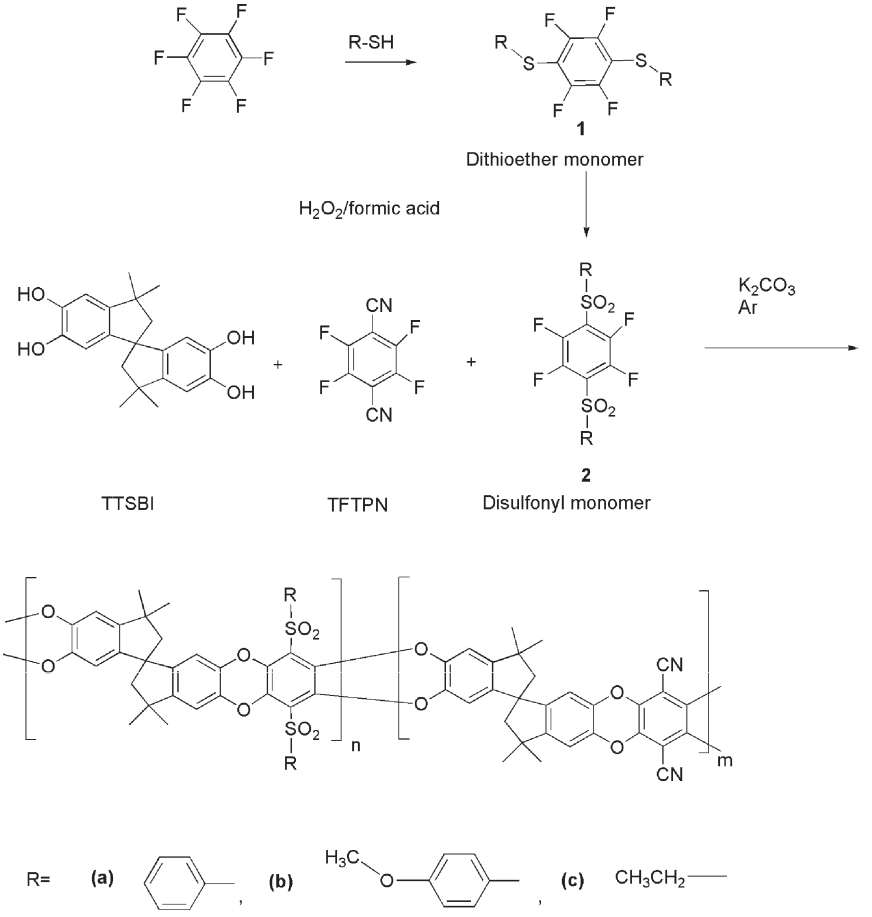

[a] DSPIM1, (a) R = Ph−; DSPIM2; (b) R = OH_3CPh−; DSPIM3, (c) R = CH_3CH_2−.

Experimental Section

Materials. Hexafluorobenzene was obtained from Apollo Scientific Ltd. and 4-methoxylbenzenethiol from Matrix Scientific. Ethanethiol, thiophenol, dimethylacetamide (DMAc), sodium hydride (60% NaH dispersion in mineral oil), formic acid, hydrogen peroxide (30% w/w H_2O_2 solution in H_2O), anhydrous potassium carbonate (K_2CO_3), and toluene were reagent grade chemicals obtained from Sigma-Aldrich and used as received. Pyridine (Sigma-Aldrich) was distilled from CaH_2. Monomer TTSBI (Sigma-Aldrich) was purified by recrystallization from methanol. Monomer TFTPN (Matrix Scientific) was purified by vacuum sublimation at 150 °C under an inert atmosphere.

Characterization Methods. The structures of the disulfone monomers and resulting disulfone-based PIMs were fully characterized using NMR spectroscopy. NMR analyses were recorded on a Varian Unity Inova spectrometer at a resonance frequency of 399.961 MHz for ^{1}H, 376.276 MHz for ^{19}F, and 100.579 MHz for ^{13}C. ^{1}H NMR, ^{19}F NMR, and ^{13}C NMR spectra were obtained from samples dissolved in $CDCl_3$ or DMSO-d_6 using a 5 mm pulsed field gradient indirect detection probe. The solvent signals ($CDCl_3$ ^{1}H 7.25 ppm, ^{13}C 77.00 ppm; DMSO-d_6 ^{1}H 2.50 ppm, ^{13}C 39.43 ppm) were used as the internal references. An external reference was used for ^{19}F NMR: $CFCl_3$ 0 ppm.

Elemental analysis was carried out with a Thermoquest CHNS-O elemental analyzer.

Molecular weights were determined using gel permeation chromatography (GPC) on a Waters Model 515 HPLC equipped with i-Styragel columns (103, 104, and 105) using THF as an eluant with polystyrene standards. Polymer thermal degradation curves were obtained from TGA (TA Instruments model 2950). Polymer samples for TGA were initially heated to 120 °C under nitrogen gas (50 mL/min) and maintained at that temperature for 1 h for moisture removal and then heated to 600 at 10 °C/min for degradation temperature measurement. Glass transition temperatures (T_g) were observed from DSC (TA Instruments model 2920), and samples for DSC were heated at 10 °C/min under a nitrogen flow of 50 mL/min, then quenched with liquid nitrogen, and reheated at 10 °C/min for the T_g measurement.

WAXD was used to investigate *d*-spacing. A Bruker AXS GADDS instrument was utilized with Cu Kα radiation of wavelength (λ) 1.54 Å. The value of the *d*-spacing was calculated by means of Bragg's law ($d = \lambda/2 \sin\theta$), using θ of the broad peak maximum.

Dense polymer films for gas permeability measurements were prepared from 1 to 2 wt % polymer solutions in chloroform. Polymer solutions were filtered through 0.45 μm poly(tetrafluoroethylene) filters and then cast into either glass or Teflon Petri dishes in a glovebox and slowly evaporated for 1 day. The films were soaked in methanol and dried in the vacuum oven at 100 °C for 24 h. The resulting membranes with thickness in the range of 60−80 μm were flexible and bright yellow. The absence of residual solvent in the films was confirmed by a weight loss test using TGA.

Permeability coefficients (*P*) of N_2, O_2, and CO_2 were determined at 25 °C with a feed pressure of 50 psig and atmospheric permeate pressure using the constant-pressure/variable-volume method. The permeate gas flow rate was measured by a mass flow meter (Agilent ADM 2000) or a bubble flowmeter. Permeability (*P*) was calculated by using the following equation:

$$P = \left(\frac{273}{T}\right)\left(\frac{dV}{dt}\right)\left(\frac{l}{\Delta pA}\right) \quad (1)$$

where dV/dt is the permeate side flow rate (cm^3/s) and T is the operation temperature (K). The membrane effective area was 9.6 cm^2.

Preparation of Disulfone Monomers 2a−c. The three thioethers **1a−c** were synthesized by modifying a known procedure.[29−31] Into a 250 mL three-neck flask equipped with a magnetic stirrer, an argon inlet, and a condenser, the appropriate thiol (54 mmol), NaH (54 mmol), and dry pyridine (15 mL) were added. The reaction mixture was cooled to −20 °C using an ice salt bath (NaCl/ice = 3:1, w/w) and stirred for 1 h. Thereafter, the resulting reaction mixture was added dropwise into hexafluorobenzene (27 mmol), and the temperature was gradually increased to room temperature. After stirring at room temperature for 30 min, the reaction mixture was refluxed for another 20 min and then poured into water. The crude product was washed with 8 N hydrochloric acid and extracted with dichloromethane and dried over $MgSO_4$. After purifying, the dithioethers (5 g) were oxidized with formic acid (15 mL) and H_2O_2 (30%, 20 g) and maintained at 100 °C for 24 h, resulting in white disulfone products (**2a−c**), which were collected and purified.

*1,2,4,5-Tetrafluoro-3,6-bisphenylsulfonylbenzene (TFBPSB) (**2a**).* The thioether **1a** was purified by column chromatography (using 1/4, v/v chloromethane/hexane). Pure product in the form of white needle crystals was obtained by recrystallization from hexane. Yield: 48%; mp: 109−110 °C. Elem. Anal. Calcd for $C_{18}H_{10}F_4S_2$ (366.4 g/mol): C, 59.01%; H, 2.75%, S 17.5%. Found: C, 58.51%; H, 2.69%; S 17.62%. ^{1}H NMR (chloroform-d) δ (ppm): 7.43−7.39 (m, 4H), 7.35−7.29 (m, 6H) ^{19}F NMR (chloroform-*d*) δ: −132.4 (s, 4F). ^{13}C NMR (chloroform-*d*) δ: 146.9 (d, J = 251 Hz, split by F), 132.5 (s), 131.0 (s), 129.4 (s), 128.1 (s), 115.3 (m).

After oxidation, the crude TFBPSB (**2a**) was recrystallized from dimethylformamide (DMF), to give white needle crystals in a yield of 81%. mp: >300 °C. Elem. Anal. Calcd for $C_{18}H_{10}F_4O_4S_2$ (430.39 g/mol): C, 50.23%; H, 2.34%, S 14.9%. Found: C, 49.57%; H, 2.042%; S 14.89%. ^{1}H NMR (DMSO-d_6) δ (ppm): 8.03 (d, J = 8.0 Hz, 4H), 7.85 (t, J = 8.0 Hz, 2H), 7.71(t, J = 8.0 Hz, 4H), ^{19}F NMR (DMSO-d_6) δ: −135.6 (s, 4F). ^{13}C NMR (DMSO-d_6) δ: 145 (dm, J = 256 Hz), 139.2 (s), 135.6 (s), 129.9 (s), 127.7 (s), 124.2 (m).

*1,2,4,5-Tetrafluoro-3,6-bis(methoxy-4-phenylsulfonyl)benzene (TFBMPSB) (**2b**).* The thioether **1b** was purified by column chromatography (using 1/2, v/v chloromethane/hexane). Pure product in the form of white flake crystals was obtained by recrystallizion from hexane. Yield: 51%; mp: 104 °C. Elem. Anal. Calcd for $C_{20}H_{14}F_4O_2S_2$ (426.45 g/mol): C, 56.33%; H, 3.31%, S 15.04%. Found: C, 55.30%; H, 3.04%; S 15.01%. ^{1}H NMR (chloroform-*d*) δ (ppm): 7.46 (d, J = 8.0 Hz, 4H), 6.84 (d, J = 8.0 Hz, 4H), 3.80 (s, 6H), ^{19}F NMR (chloroform-*d*) δ: −133.7 (s, 4F). ^{13}C NMR (chloroform-*d*) δ: 160.2 (s), 146.7 (dm, J = 251 Hz), 134.8 (s), 122.4 (s), 114.8 (s), 109.8 (m), 55.3 (s).

After oxidation, the crude TFBMPSB (**2b**) was recrystallized from DMF, to give white needle crystals in 78% yield. mp: >300 °C. Elem. Anal. Calcd for $C_{20}H_{14}F_4O_6S_2$ (490.45 g/mol): C, 48.98%; H, 2.88%, S 13.08%. Found: C, 48.38%; H, 3.047%; S 13.01%. ^{1}H NMR (DMSO-d_6) δ (ppm): 7.95 (dd, J = 8.0 Hz, 4H), 7.20 (dd, J = 8.0 Hz, 4H), 3.86 (s, 6H), ^{19}F NMR (DMSO-d_6) δ: −136.2 (s, 4F). ^{13}C NMR (DMSO-d_6) δ: 161.3 (s), 144.5 (dm, J = 251 Hz), 133.3 (s), 130.3 (s), 123.1 (m), 115.2 (s), 54.91 (s).

*1,2,4,5-Tetrafluoro-3,6-bis(ethylsulfonyl)benzene (TFBESB) (**2c**).* The 1,4-bis(ethylthio)-2,3,5,6-tetrafluorobenzene (**1c**) was oxidized without purification. The crude disulfone was recrystallized in DMF and toluene to give white needles of TFBESB in 72% yield. mp: 239 °C. Elem. Anal. Calcd for $C_{10}H_{10}F_4O_4S_2$ (334 g/mol): C, 35.93%; H, 3.02%, S 19.18%. Found: C, 35.65%; H, 2.91%; S 18.65%. ^{1}H NMR (DMSO-d_6) δ (ppm): 3.61 (q, J = 8.0 Hz, 4H), 1.27 (t, J = 8.0 Hz, 6H) ^{19}F NMR (DMSO-d_6) δ: −135 (s, 4F). ^{13}C NMR (DMSO-d_6) δ: 142.4 (dm, J = 251 Hz), 129.94 (m), 51.2 (s), 6.4 (s).

Preparation of PIM-1 as a Comparative Sample. PIM-1 was synthesized by a known procedure in DMAc at an elevated temperature of 160 °C.[26]

Preparation of PIM Ladder Polymers Containing Disulfonyl Groups (DSPIM1−3). DSPIMs-100, DSPIMs-50, and DSPIMs-33 were synthesized by copolymerization of TTSBI, TFTPN, and disulfone monomers using a procedure similar to that of PIM-1.[26] The homopolymers are referred to as DSPIMs-100, and the copolymers are identified as DSPIMs-50 and DSPIMs-33, where PIM stands for polymer of intrinsic microporosity, DS stands for disulfonyl groups, and suffixes -100, -50, and -33 refer to the disulfone to TTSBI ratio in the copolymers.

Into a 100 mL three-necked flask equipped with a magnetic stirrer, an argon inlet, and a Dean−Stark trap, TFTPN, TTSBI and disulfone monomers, anhydrous K_2CO_3, DMAc, and toluene were added. The mixture was refluxed at 160 °C for 40−60 min, and then the resulting viscous polymer solution was precipitated into methanol. A yellow flexible threadlike polymer was obtained. The polymer product was dissolved into chloroform and reprecipitated from methanol. The resulting polymer was refluxed for several hours with deionized water and dried in the vacuum oven at 100 °C for 48 h.

Results and Discussion

Monomer Syntheses. The syntheses of disulfone monomers comprised two steps: aromatic nucleophilic substitution reaction and oxidation (Scheme 1). Different from the known procedure,[29−31] the sodium thiolate and pyridine mixture was added dropwise to hexafluorobenzene at −20 °C instead of adding hexafluorobenezene into sodium thiolate and pyridine mixture at reflux temperature (above 115 °C). Hexafluorobenzene easily reacts with thiol groups under basic conditions by a aromatic nucleophilic substitution reaction, especially at an elevated temperature. Even at room temperature, the addition of more than a two molar ratio of hexafluorobenzene to sodium thiolate still resulted in the formation of 1,4-difluorotetrathiobenzene compounds. According to our modified synthesis method, tetrathioether compounds were successfully avoided, and the three dithioether monomer precursors (**1a−c**) were obtained in good yield. It was also found that the oxidation of thio groups was not complete when using excess H_2O_2 in heterogeneous formic acid suspension at 100 °C for 1 h. After 1 h oxidation, only 20−30% thio groups were oxidized (observed from ^{1}H NMR spectra), which is different from the previous work.[30] In general, the oxidation of dithio compounds is completed only after at least 24 h at 100 °C due to the poor solubility of partially oxidized compounds. Monomer dithio precursors (**1a**, **1b**) were purified before oxidation, but the diethylthio precursor (**1c**) for monomer TFBESB (**2c**) was oxidized without prior purification because the resulting disulfone monomer was more easily purified by recrystallization.

Polymerization. The three series of ladder DSPIM copolymers and homopolymers containing disulfonyl groups with or without −CN groups, respectively, were prepared via the S_NAr polycondensation reaction using various feed ratios of TTSBI/TFTPN/disulfone monomers. The compositions and molecular weights of the polymers are listed in Table 1.

According to the polycondensation reaction mechanism for poly(arylene ether)s, high temperature and high concentration are favorable for increasing the solubility of phenoxide salt and growing the polymer chain; hence, the occurrence of cyclic oligomers and cross-linked structures can be effectively reduced. A new polymerization procedure

Table 1. Compositions and Molecular Weights of DSPIM1−3 and PIM-1

polymers	TTSBI (molar ratio)	disulfone monomer (molar ratio)	TFTPN (molar ratio)	M_n	M_w	M_w/M_n
DSPIM1-100	1	1[a]	0	66 000	413 000	6.2
DSPIM1-50	2	1[a]	1	63 000	453 000	7.1
DSPIM1-33	3	1[a]	2	43 000	187 000	4.3
DSPIM2-100	1	1[b]	0	58 000	625 000	10.8
DSPIM2-50	2	1[b]	1	46 000	350 000	7.6
DSPIM2-33	3	1[b]	2	41 000	84 000	2.1
DSPIM3-100	1	1[c]	0	49 000	478 000	9.7
DSPIM3-50	2	1[c]	1	52 000	421 000	8.1
DSPIM3-33	3	1[c]	2	95 000	489 000	5.1
PIM-1	1	0	1	58 000	193 000	3.3

[a] Monomer **2a**. [b] Monomer **2b**. [c] Monomer **2c**.

for PIM-1 and related PIM copolymer structures (TFMPSPIMs) was recently reported using high monomer concentrations (>25 wt %) and at elevated temperatures (160 °C).[26] Excess toluene was introduced into the reaction not only to remove water but also to provide solubility enhancement of the polymer. The reactions proceeded smoothly with no evidence of cross-linking.[26] In contrast with the previous work, the polycondensation of the present DSPIMs are different from PIM-1 and TFMPSPIMs. In the aromatic nucleophilic substitution reaction, there are two main factors influencing the substitution occurring in the aromatic system: (a) electronic activation and deactivation and (b) steric deactivation. In general, it can be assumed that every substituent ortho to the substitution site has some steric effect on the reaction rate. However, for the majority of the data reported before, the electronic effect of the electron-donating or -withdrawing group appears to be far more pronounced than the steric effect.[32] It is well-known that electron-withdrawing groups have different electronic activation, in the sequence of $-SO_2R > -CF_3 > -CN$.[33] Because PIMs have a rigid ladder structure, which is different from linear flexible polymers, steric deactivation may have a more pronounced effect. In the first substitution reaction (I) shown in Figure 1, wherein a phenoxide nucleophile displaces a fluorine atom, the steric effect may not be obvious because the electrophile can attack perpendicularly to the ring.[33] Comparing three tetrafluoro-based monomers, the initial substitution reactions will occur at the ortho-activated fluorine atom (atom 1) near $-SO_2R$ or $-CN$ groups. When the second substitution reaction (II) forms the dibenzodioxane-based structure, the $Ar-O^-K^+$ has to attack the fluorine atom (atom 2) on the same side, from the horizontal direction, resulting in a quasi-planar dioxane ring. Therefore, steric effects may become significant for dioxane ring formation in PIMs. If the electron-withdrawing groups are not too bulky, such as $-CN$ and $-CF_3$, the dibenzodioxane ring structure will be formed relatively easily.[26] On the other hand, $-SO_2R$ is larger so as to hinder efficient electrophilic attack from the horizontal direction. Hence, under the high concentration reaction conditions used, after substitution reaction I occurs, there may be a competing substitution reaction I (perpendicular direction) on atom 1 of another monomer rather than the desired dibenzodioxane ring formation brought about by substitution reaction II (horizontal direction) on atom 2 of the same monomer. However, if reaction conditions are used whereby the concentration of disulfone monomer is low, dibenzodioxane ring formation is more likely to occur after the initial substitution reaction I due to the dilution effect. Meanwhile, the reactivity of comonomer TFTPN is not as high as the disulfone-based monomers. Hence, with a progressively decreasing molar ratio of disulfone-based

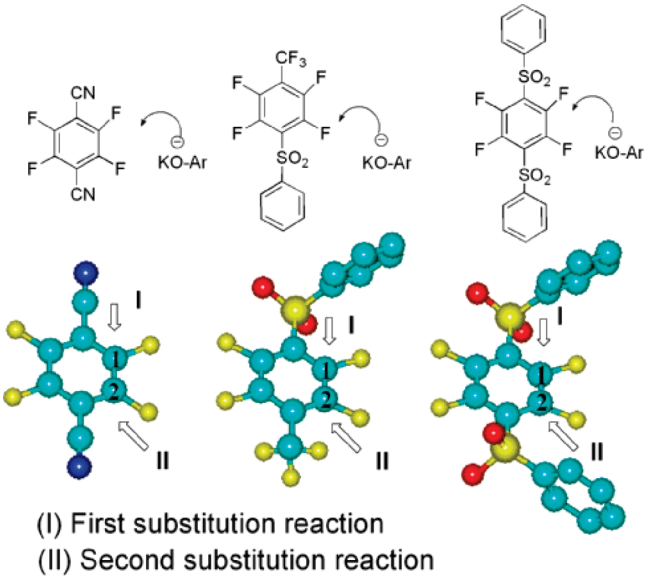

Figure 1. Aromatic nucleophilic substitution reaction of tetrafluoro monomers.

monomer to TTSBI, polydispersity is observed to decrease. The GPC curves of DSPIM-100 homopolymers (not shown) reveal several shoulder peaks in the high molecular weight region along with the main peak. A minor gel fraction indicated that some cross-linking had occurred during the reaction. With decreasing ratios of disulfone-based monomers, only negligible gel formation was observed. The M_n of all three DSPIMs-33 copolymers (in Table 1) are above 41 000 Da, and the polydispersity indices are in the range of 2−5. Although the polydispersity indices of DSPIMs-33 are somewhat higher than typical PIM-1 and PSTFPIM obtained under the same conditions,[26] the quality of the copolymers was still adequate to provide solution-cast robust free-standing films for gas permeability measurements.

NMR Analysis. All three DSPIM-50 copolymers were fully characterized by ^1H and ^{19}F NMR spectroscopy. The ^1H spectra of DSPIM-50 copolymers were obviously similar to those of PIM-1 due to their identical TTSBI and TFTPN monomer content. The additional signals due to the different disulfone monomer were readily assigned in ^1H NMR. Furthermore, the experimental ratio of intensity values for aromatic protons H-8, -11, or -13 compared with aliphatic protons H-2,3 was found to be exactly as expected; for example, the spectra of the DSPIM-50 displayed in Figure 1 all had proton ratios of exactly 4H:8H per repeat unit.

A three-dimensional representation of the PIM polymer structures explains better what is observed in ^1H NMR

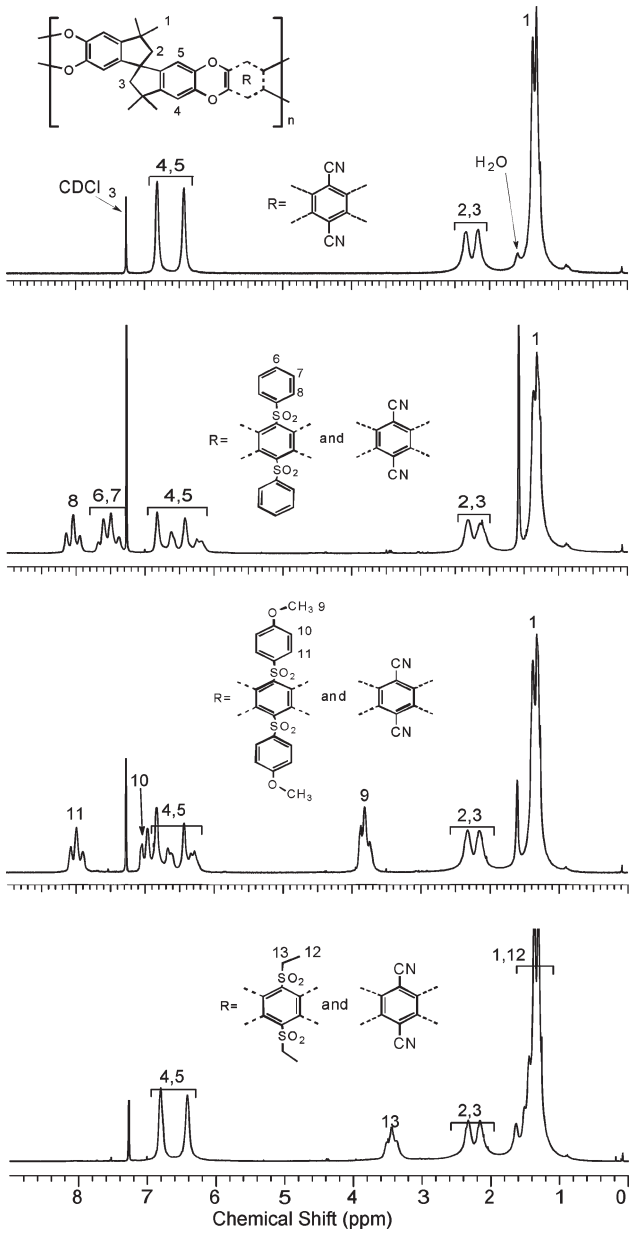

Figure 2. ^{1}H NMR spectra of PIM-1 (top), DSPIM1-50, DSPIM2-50, and DSPIM3-50.

spectroscopy. In 3-D it is clear that one of the methyl groups is within very close proximity of H-5, and therefore the electron cloud of the CH_3 group shields this proton; hence its very low chemical shift (6.4 ppm) for an aromatic proton. From the H-4 perspective, the two methyl groups are more distant; hence, less shielding and the higher chemical shift (6.8 ppm) is observed. This combines to explain why the methyl groups (H-1) do not appear as a singlet but as two singlets because they are not equivalent in a 3-D representation. The same principle also applies to H-2 and H-3.

The H-4 and H-5 protons appear at the same position for both PIM-1 and DSPIM3-50 because the pendant groups, $-$CN and $-SO_2CH_2CH_3$, respectively, are small and sufficiently distant from the aromatic protons that they have little effect on them. On the other hand, the two PIM copolymers DSPIM1-50 and DSPIM2-50 have bulky pendant phenyl groups with aromatic annular effects (ring current). These groups cause H-4 and H-5 to appear at different chemical shifts. Hence, multiple H-4 and H-5 signals appear for DSPIM1-50 and DSPIM2-50 but not for PIM-1 and DSPIM3-50.

Table 2. Thermal Properties of the DSPIM1−3 Series and PIM-1

polymers	T_d (°C)[a]	T_d (°C)[b]	T_{d5} (°C)[c]	RW (%)[d]
DSPIM1-100	346.5	421.2	421.5	53.5
DSPIM1-50	372.3	451.91	449.84	63.0
DSPIM1-33	407.7	475.2	484.67	63.7
DSPIM2-100	329.7	417.2	412.5	51.0
DSPIM2-50	361.8	447.29	447.65	59.0
DSPIM2-33	384.7	464.9	475.92	62.5
DSPIM3-100	304.0	357.1	357.9	40.0
DSPIM3-50	317.0	398.46	376.33	48.0
DSPIM3-33	362.9	423.9	434.92	61.5
PIM-1	429.6	492.6	495.4	68.0

[a] Actual onset temperature of decomposition. [b] Extrapolated onset temperature of decomposition measured by TGA. [c] Five percent weight loss temperature measured by TGA. [d] Residue weight at 600 °C under N_2.

Finally, the ^{19}F NMR spectra (not shown) were collected for all DSPIMs homo- and copolymers. It is worthwhile mentioning that no aromatic F signals were observed.

Thermal Analysis. Thermal analyses for DSPIMs and PIM-1 were carried out, and the results are summarized in Table 2. All polymers were amorphous and had no discernible T_g up to their decomposition temperatures (> 317 °C). TGA experiments showed that all polymers had excellent thermal stabilities, and the actual onset temperature of decomposition in nitrogen ranged from 317 to 407 °C. There was also some trend between the decomposition temperature and the monomer ratio. Generally, polymers with $-SO_2Ar$ groups have high thermal stability. However, the $-$CN side group can enhance the thermal properties due to strong dipolar interactions. With increasing molar ratios of $-$CN groups in the DSPIMs, the onset of thermal decomposition also increased, as shown in Table 2. However, DSPIM homopolymers and copolymers all showed very good thermal stability even after the replacement of $-$CN with $-SO_2R$ groups.

Gas Transport Properties. *Free Volume Analysis.* The fractional free volume (FFV) is calculated using eqs 2, 3, and 4:[26]

$$\mathrm{FFV} = (V - V_0)/V \tag{2}$$

$$V = M/\rho \tag{3}$$

$$V_0 = 1.3V_w \tag{4}$$

where V is the total molar volume of the monomer unit (cm^3/mol), M the molar mass (g/mol) of the monomer unit, and ρ the density of the film (g/cm^3), which was determined experimentally (determined by measurements of the weight in air and in the ethanol). V_0 is the volume occupied by the chains (cm^3/mol). V_0 is assumed to be impermeable for diffusing gas molecules. V_w is the van der Waals volume calculated using the group contribution method of Bondi.[34−36] According to Bondi, a good approximation of relation between V_0 and V_w is given by eq 4, and the results are given in Table 3. The FFV varied from a minimum of 0.09 for DSPIM2-100 to a maximum of 0.26 for PIM-1. The FFV of DSPIM-33 copolymers is around 0.20. Compared to PIM-1, DSPIM-33 copolymers are able to pack space more efficiently.

X-ray Diffraction Studies. WAXD revealed that DSPIM-33 copolymers were amorphous. Two main broad peaks were observed for all polymers. According to Bragg's law, the peak representing 4.9 Å might be attributed to the

Table 3. Physical Properties of DSPIM1−3 Series and PIM-1

polymers	ρ, g/cm^3	V, cm^3/g	M, g/mol	V_w, cm^3/mol	$V - V_0$, cm^3/g	FFV
DSPIM1-100	1.356	0.737	690.78	349.2	0.080	0.11
DSPIM1-50	1.207	0.829	575.63	297.8	0.156	0.19
DSPIM1-33	1.187	0.842	537.25	280.6	0.163	0.19
DSPIM2-100	1.369	0.730	750.83	382.4	0.068	0.09
DSPIM2-50	1.234	0.810	605.66	314.4	0.135	0.17
DSPIM2-33	1.198	0.835	557.26	291.7	0.155	0.19
DSPIM3-100	1.325	0.755	594.70	305.3	0.088	0.12
DSPIM3-50	1.214	0.824	527.59	275.8	0.144	0.18
DSPIM3-33	1.162	0.861	505.22	266.0	0.177	0.21
PIM-1	1.063	0.94	460.48	246.3	0.244	0.26

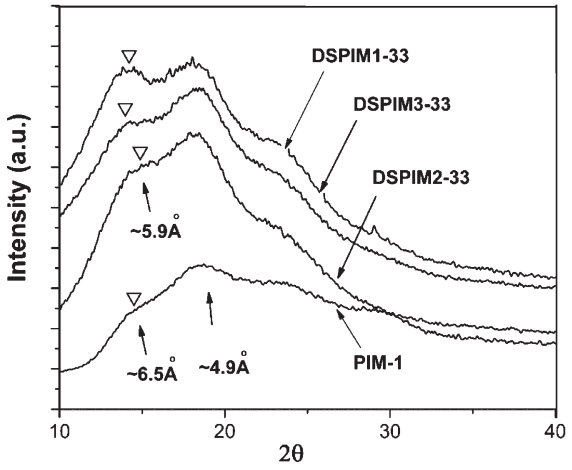

Figure 3. WAXD of DSPIM-33 copolymers and PIM-1.

chain-to-chain distance of space-efficiently packed chains. On the other hand, the second peak found at a *d*-spacing of about 6.5 Å corresponds to more loosely packed polymer chains.[12] As shown in Figure 3, the *d*-spacing is 5.9 Å for DSPIM2-33 and 6.5 Å for PIM-1. It becomes larger with decreasing the size of disulfonyl groups in the main chain, suggesting that the different disulfonyl groups affect polymer chain packing. The increasing size of disulfonyl groups leads to lower FFV due to interchain space filling.

Gas Permeability. Although free-standing films of the all the copolymers and homopolymers could be prepared, gas permeability measurements were conducted only on the DSPIM-33 copolymers with low polydispersity. Single-gas permeability coefficients (P) for O_2, N_2, and CO_2 were determined at 25 °C for dense, isotropic polymer films (PIM-1 and DSPIM-33 copolymers), and a summary of these P values and ideal selectivities for various gas pairs are shown in Table 4. In comparison with PIM-1, the newly synthesized DSPIM-33 copolymers exhibited higher selectivity, coupled with expected reductions in gas permeabilities. The selectivities for O_2/N_2 and CO_2/N_2 were in the range of 3.7−4.2 and 16−23, respectively. These results agree with the general tendency for gas permeation through polymer membranes—higher O_2 and CO_2 permeability is gained at the cost of lower selectivity and vice versa.

Robeson proposed upper bound performance lines for this trade-off relationship between permeability and selectivity.[38,39] It is especially noteworthy that the O_2 permeation data of DSPIMs-33 were all positioned above the 1991 Robeson upper bound line, as shown in Figure 4. The high permeability and selectivity of O_2 and CO_2 of the DSPIM-33 copolymers can be ascribed to the presence of both nitrile and disulfone groups, which are sufficiently polar. While these pendent groups do not increase the FFV or reduce chain packing, they increase chain stiffness and likely have an

Table 4. Gas Permeabilities and Selectivities of DSPIM1-33, DSPIM2-33, DSPIM3-33, and PIM-1

	P (barrer[a])			α[b]	
polymers	O_2	N_2	CO_2	O_2/N_2	CO_2/N_2
DSPIM1-33	322	88	1408	3.7	16
DSPIM2-33	216	52	1077	4.2	21
DSPIM3-33	369	93	2154	3.9	23
PIM-1	1133	353	5366	3.2	15

[a] Permeability coefficients measured at 25 °C; feed pressure: 50 psig; permate pressure: 0 psig. 1 barrer = 10^{-10} cm^3 (STP) cm/(cm^2 s cmHg). [b] Selectivity $\alpha = P_a/P_b$.

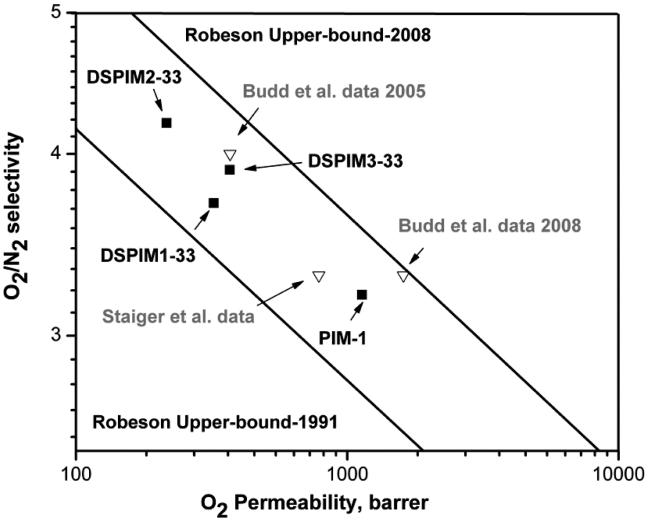

Figure 4. Trade-off between O_2 permeability and O_2/N_2 selectivity for DSPIM1-33, DSPIM2-33, DSPIM3-33, and PIM-1 membranes relative to the Robeson's upper bound.[38,39] ▽: Data from Budd et al. were reported (2005) at 200 mbar (2.90 psia) feed pressure at 30 °C and (2008) at 1 atm (14.7 psig) feed pressure at 23 °C.[18,37] ▽: Data from Staiger et al. were reported at 4 atm (58.8 psia) feed pressure at 35 °C.[40]

effect of interchain space filling, which results in an increase in selectivity. On the other hand, the permeability decreases by enlarging the size of pendent groups on PIMs. In summary, the three disulfone groups have different effects on space filling and interchain packing. The permeability and selectivity of PIMs can be tuned by the size of pendent groups. For example, ethyl-substituted DSPIM3-33 has the best combination of permeability coupled with selectivity for O_2/N_2 and CO_2/N_2 among the three DSPIM-33 series. Future studies will focus on preparing PIMs with higher performance by modifying side groups and/or tuning the size or ratio of pendant groups.

Molecular Modeling. Molecular modeling analyses of DSPIM-100 homopolymers and PIM-1 with two repeat unit lengths were performed by using HyperChem 7.0 software

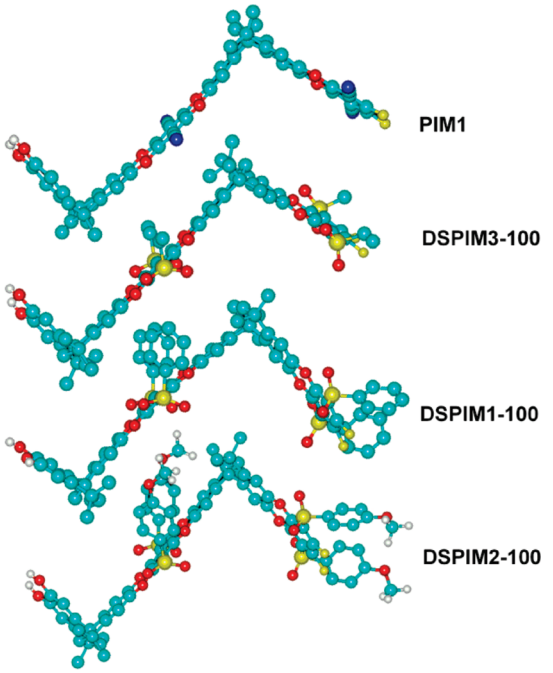

Figure 5. Visual models of the PIM-1 and DSPIM-100 homopolymers as calculated with energy minimization.

for studying the effect on geometry and steric interaction of disulfonyl groups on the polymer chains. In Figure 5, a visual indication of major conformational changes in the polymers was obtained by the calculation results of geometry optimization with energy minimization using the AMBER method. The chains of PIM-1 with −CN pendent groups shown for comparison are relatively spiro-zigzag linear and regular ladder structure, which would lead to less chain packing. Compared with PIM-1, DSPIMs showed a similarly unperturbed coil conformation. Although disulfonyl groups are more bulky than the −CN group, they do not change the overall spiro-zigzag ladder chain structure and also do not take more intermolecular space. In addition, the rigidity of the ladder polymers chain with disulfonyl groups can be enhanced by hindering bond distortions within the ladder chain; hence, selective diffusion ability can be enhanced. The different pendent groups also act as the interchain space fillers with different size, which results in a decrease in permeability in a diverse way. Thus, the gas transport properties of DSPIMs can be tuned by introducing the different side groups on the main ladder chains. The molecular modeling is in agreement with the gas permeability and selectivity data and helps to explain the observed changes in gas selectivity of DSPIM-33 copolymers versus PIM-1.

Conclusions

Three novel disulfone-based monomers derived from readily available hexafluorobenzene and thiol were synthesized and fully characterized for the preparation of PIM homopolymers and copolymers. Among them, 1,2,4,5-tetrafluoro-3,6-bis(methoxy-4-phenzylsulfonyl)benzene ((**2b**) TFBMPSB) and 1,2,4,5-tetrafluoro-3,6-bis(ethylsulfonyl)benzene ((**2c**) TFBESB) are reported as new compounds. Three series of DSPIMs (DSPIM1−3) extend the possible structures of PIM ladder polymers having high molecular weight beyond those reported previously. The polymerizations were run under high temperature and high concentration conditions in order to minimize the formation of cyclic species and cross-linking. The small amount of cross-linking observed in disulfone-based homopolymers was explained by possible electronic and steric effects for disulfone monomers. The DSPIM series had high T_d in the range of 304−407 °C. The intrinsic microporosity of these polymers was supported by the FFV data, X-ray diffraction measurements, gas permeability measurements, and molecular modeling. Dense films fabricated from DSPIM-33 copolymers had higher O_2/N_2 and CO_2/N_2 selectivities than PIM-1 made under similar conditions that combine with gas permeabilities to exceed the Robeson upper bound. The incorporation of disulfonyl side groups into PIM structures increases selectivity. In addition, the gas permeabilities and selectivities of DSPIMs can be tuned by the size and nature of the pendant side chains and the copolymer ratio.

Acknowledgment. This work was supported primarily by the Climate Change Technology and Innovation Initiative, Greenhouse Gas project (CCTII, GHG). Partial support was also provided by the U.S. Department of Energy (SBIR Contract DE-FG02-05ER84243). The authors are grateful to Ms. Patarachao Bussaraporn for the WAXD measurements.

References and Notes

(1) Davankov, V. A.; Tsyurupa, M. P. *React. Polym.* **1990**, *13*, 27–42.
(2) Tsyurupa, M. P.; Davankov, V. A. *React. Funct. Polym.* **2002**, *53*, 193–203.
(3) Budd, P. M.; Ghanem, B.; Msayib, K.; McKeown, N. B.; Tattershall, C. *J. Mater. Chem.* **2003**, *13*, 2721–2726.
(4) McKeown, N. B.; Gahnem, B.; Msayib, K. J.; Budd, P. M.; Tattershall, C. E.; Mahmood, K.; Tan, S.; Book, D.; Langmi, H. W.; Walton, A. *Angew. Chem., Int. Ed.* **2006**, *45*, 1804–1807.
(5) Webster, O. W.; Gentry, F. P.; Farlee, R. D.; Smart, B. E. *Makromol. Chem., Macromol. Symp.* **1992**, *54*, 477–482.
(6) Urban, C.; McCord, E. F.; Webster, O. W.; Abrams, L.; Long, H. W.; Gaede, H.; Tang, P.; Pines, A. *Chem. Mater.* **1995**, *7*, 1325–1332.
(7) Wood, C. D.; Tan, B.; Trewin, A.; Niu, H. J.; Bradshaw, D.; Rosseinsky, M. J.; Khimyak, Y. Z.; Campbell, N. L.; Kirk, R.; Stockel, E.; Cooper, A. I. *Chem. Mater.* **2007**, *19*, 2034–2048.
(8) McKeown, N. B.; Hanif, S.; Msayib, K.; Tattershall, C. E.; Budd, P. M. *Chem. Commun.* **2002**, 2782–2783.
(9) Masuda, T.; Isobe, E.; Higashimura, T.; Takada, K. *J. Am. Chem. Soc.* **1983**, *105*, 7473–7474.
(10) Nagai, K.; Masuda, T.; Nakagawa, T.; Freeman, B. D.; Pinnau, I. *Prog. Polym. Sci.* **2001**, *26*, 721–798.
(11) Tanaka, K.; Okano, M.; Toshino, H.; Kita, H.; Okamoto, K. I. *J. Polym. Sci., Polym. Phys.* **1992**, *30*, 907–914.
(12) Weber, J.; Su, Q.; Antonietti, M.; Thomas, A. *Macromol. Rapid Commun.* **2007**, *28*, 1871–1876.
(13) Yu, A.; Shantarovich, V.; Merkel, T. C.; Bondar, V. I.; Freeman, B. D.; Yampolskii, Y. *Macromolecules* **2002**, *35*, 9513–9522.
(14) Dai, Y.; Guiver, M. D.; Robertson, G. P.; Kang, Y. S. *Macromolecules* **2005**, *38*, 9670–9678.
(15) Dai, Y.; Guiver, M. D.; Robertson, G. P.; Kang, Y. S.; Lee, K. J.; Jho, J. Y. *Macromolecules* **2004**, *37*, 1403–1410.
(16) Park, B. H.; Jung, C. H.; Lee, Y. M.; Hill, A. J.; Pas, S. J.; Mudie, S. T.; Van Wagner, V. E.; Freeman, B. D.; Cookson, D. J. *Science* **2007**, *318*, 254−258.
(17) (a) McKeown, N. B.; Budd, P. M. *Chem. Soc. Rev.* **2006**, *35*, 675–683. (b) Budd, P. M.; Elabas, E. S.; Ghanem, B. S.; Makhseed, S.; McKeown, N. B.; Msayib, K. J.; Tattershall, C. E.; Wong, D. *Adv. Mater.* **2004**, *16*, 456–459.
(18) Budd, P. M.; Msayib, K. J.; Tattershall, C. E.; Reynolds, K. J.; McKeown, N. B.; Fritsch, D. *J. Membr. Sci.* **2005**, *251*, 263–269.
(19) Ghanem, B.; McKeown, N. B.; Harris, K. D. M.; Pan, Z.; Budd, P. M.; Butler, A.; Selbie, J.; Book, D.; Walton, A. *Chem. Commun.* **2007**, 67–69.
(20) Budd, P. M.; Butler, A.; Selbie, J.; Mahmood, K.; McKeown, N. B.; Ghanem, B.; Msayib, K.; Book, D.; Walton, A. *Phys. Chem. Chem. Phys.* **2007**, *9*, 1802–1808.
(21) McKeown, N. B.; Budd, P. M.; Book, D. *Macromol. Rapid Commun.* **2007**, *28*, 995–1002.
(22) Maffei, A. V.; Budd, P. M.; McKeown, N. B. *Langmuir* **2006**, *22*, 4225–4229.
(23) Ghanem, B.; McKeown, N. B.; Budd, P. M.; Fritsch, D. *Macromolecules* **2008**, *41*, 1640–1646.

(24) Budd, P. M.; Ghanem, B. S.; Makhseed, S.; McKeown, N. B.; Msayib, K. J.; Tattershall, C. *Chem. Commun.* **2004**, 230–231.
(25) Kricheldorf, H. R.; Fritsch, D.; Vakhtangishvili, L.; Lomadze, N.; Schwarz, G. *Macromolecules* **2006**, *39*, 4990–4998.
(26) (a) Du, N.; Robertson, G. P.; Song, J.; Pinnau, I.; Thomas, S.; Guiver, M. D. *Macromolecules* **2008**, *41*, 9656–9662. (b) Du, N.; Robertson, G. P.; Pinnau, I.; Thomas, S.; Guiver, M. D. *Macromol. Rapid Commun.* **2009**, *30*, 584–588.
(27) McKeown, N. B.; Budd, P. M.; Msayib, K.; Ghanem, B. Microporous polymer material, WO 2005/012397 A2.
(28) Paul, D. R.; Yampol'skii, Y. *Polymeric Gas Separation Membranes*; CRC Press: Boca Raton, FL, 1994; p 107.
(29) Kulka, M. *J. Org. Chem.* **1959**, *24*, 235–237.
(30) Robson, P.; Smith, T. A.; Stephens, R.; Tatlow, J. C. *J. Chem. Soc.* **1963**, *7*, 3692–3703.
(31) Langille, K. R.; Peach, M. E. *J. Fluorine Chem.* **1972**, 407–414.
(32) Bunnett, J. F.; Zahler, R. E. *Chem. Rev.* **1951**, *49*, 273–412.
(33) March, J. *Advanced Organic Chemistry*; McGraw-Hill: New York, 1970; p 253.
(34) Bondi, A. *J. Phys. Chem.* **1964**, *68*, 441–451.
(35) Van Krevelen, D. W. *Properties of Polymers: Their Correlation with Chemical Structure; Their Numerical Estimation and Prediction from Additive Group Contributions*; Elsevier: Amsterdam, 1990.
(36) Lee, W. M. *Polym. Eng. Sci.* **1980**, *20*, 65–79.
(37) Budd, P. M.; McKeown, N. B.; Ghanem, B. S.; Msayib, K. J.; Fritsch, D.; Starannikova, L.; Belov, N.; Sanfirova, O.; Yampolskii, Y.; Shantarovich, V. *J. Membr. Sci.* **2008**, *325*, 851–860.
(38) Robeson, L. M. *J. Membr. Sci.* **1991**, *62*, 165–185.
(39) Robeson, L. M. *J. Membr. Sci.* **2008**, *320*, 390–400.
(40) Staiger, C. L.; Pas, S. J.; Hill, A. J.; Cornelius, C. *J. Chem. Mater.* **2008**, *20*, 2606–2608.